Integrity Risk of Kalman Filter-Based RAIM

Mathieu Joerger and Boris Pervan,
Illinois Institute of Technology

BIOGRAPHY

Dr. Mathieu Joerger obtained a Master in Mechatronics from the National Institute of Applied Sciences in Strasbourg, France, in 2002. He pursued studies in Mechanical and Aerospace Engineering at the Illinois Institute of Technology (IIT) in Chicago, where he earned a M.S. degree in 2002, and a Ph.D. in 2009. He is the 2009 recipient of the ION Bradford Parkinson award, which honors outstanding graduate students in the field of GNSS. Mathieu is currently a research associate at the Illinois Institute of Technology, working on multi-sensor integration, on sequential fault-detection for multi-constellation navigation systems, and on differential and relative RAIM for shipboard landing of military aircraft.

Dr. Boris Pervan is Professor of Mechanical and Aerospace Engineering at the Illinois Institute of Technology (IIT), where he conducts research on high-integrity satellite navigation systems. Prof. Pervan received his B.S. from the University of Notre Dame, M.S. from the California Institute of Technology, and Ph.D. from Stanford University. Prior to joining the faculty at IIT, he was a spacecraft mission analyst at Hughes Space and Communications Group and was project leader at Stanford University for GPS LAAS research and development. He was the recipient of the Mechanical and Aerospace Dept. Excellence in Research Award (2007), IIT/Sigma Xi Excellence in University Research Award (2005), University Excellence in Teaching Award (2005), Ralph Barnett Mechanical and Aerospace Dept. Outstanding Teaching Award (2002, 2009), IEEE Aerospace and Electronic Systems Society M. Barry Carlton Award (1999), RTCA William E. Jackson Award (1996), Guggenheim Fellowship (Caltech 1987), and Albert J. Zahm Prize in Aeronautics (Notre Dame 1986). He is currently Editor of the ION journal Navigation.

ABSTRACT

This paper introduces a new Kalman filter-based receiver autonomous integrity monitoring (RAIM) method for navigation systems that require measurement filtering over time (such as integrated GPS/INS navigation or carrier phase positioning). In contrast with existing sequential fault-detection algorithms, the proposed method is computationally efficient, straightforward to implement, and most importantly, it enables direct integrity risk evaluation. First, the Kalman filter-based detection test-statistic is established as a sum of generalized non-central chi-square distributed random variables. This test statistic can be recursively updated in real-time by simply adding the current-time Kalman filter residual contribution to a previously computed weighted norm of past-time residuals. Second, the test statistic is proved to be stochastically independent from the state estimate error, which enables to rigorously quantify the integrity risk (the integrity risk is defined as the probability of faults going undetected while causing hazardous information). The Kalman filter-based RAIM method is presented in a general formulation applicable to linear dynamic systems. The performance of the new detection method is illustrated and analyzed in a benchmark application of aircraft precision approach, where differential GPS and Galileo code and carrier phase measurements are filtered for positioning and floating cycle ambiguity estimation.

I. INTRODUCTION

This paper describes the design, analysis and evaluation of a new Kalman filter-based receiver autonomous integrity monitoring (RAIM) method. In contrast with existing sequential fault-detection algorithms, the proposed method enables direct and rigorous integrity risk computation using a carefully-derived test statistic, which can be recursively updated. The new method is expressed in a general formulation for a linear dynamic system.

The Kalman filter (KF) is a recursive estimator that exploits information from both the measurements and the system's dynamic model. It is used in navigation applications, for example to process GNSS carrier phase observations where cycle ambiguities are known to be constants for as long as the signal is continuously tracked (in this case, the dynamic model accounts for the constant biases). Kalman filters are also employed to accomplish tight integration of GPS with dead-reckoning sensors (such as inertial navigation systems or INS) [1], with laser scanner observations [2], with prior knowledge on receiver clock time-variations [3], and with vehicle

dynamic models [4]. The KF is widely implemented because it recursively generates optimal current-time state estimates, which maximizes current-time accuracy and fault-free integrity performance.

In addition, for high-integrity applications, the sequence of measurements must be monitored against rare event faults (such as user equipment and satellite failures). Despite multiple prior approaches (reviewed below), there is currently no widely used sequential fault-detection algorithm. One major shortcoming of published methods is their limited ability to accurately evaluate the integrity risk.

Integrity risk evaluation is essential in establishing the system's availability, which constitutes the overall navigation performance measure. In practice, integrity risk evaluation is needed when designing navigation systems to achieve required levels of integrity, and it is needed operationally to predict if a mission can be safely initiated. Evaluating the integrity risk includes both assessing the fault detection capability and quantifying the impact of undetected faults on state estimate errors.

Residual-based 'snapshot RAIM' [5] [6] does provide the means for rigorous integrity risk computation. Most existing implementations of RAIM are 'snapshot' detection schemes that assume redundant observations at one epoch of interest. Snapshot RAIM is a natural choice for punctual (e.g., code-based) position fixes, but it is insufficient for sequential implementations.

Sequential detection approaches have also been investigated [7], including multiple-hypotheses [8] [9] [10] and innovation-based methods [11] [12] [13]. These procedures quantify the fault-detection capability without regard to the fault's impact on state estimates. In this case, for navigation applications, all undetected faults should be considered hazardous, which is an overly conservative assumption that would yield poor availability performance.

Additional references are cited in [14], where the extensive literature review of research efforts carried out over the past two decades demonstrates the lively and sustained interest for real-time sequential fault detection methods, especially in the context of tightly coupled GPS/INS. The most elaborate sequential fault-detection algorithms provide protection level equations, which are measures of the integrity risk in terms of position-domain bounds. But these protection levels are still conservative [15] [16] [17] and they require computationally expensive processing procedures. For example, the solution-separation approach to sequential implementations uses banks of KF [18], whose number increases as the number of epochs in the time-sequence increases.

In response, in this work, we derive a computationally-efficient KF-based RAIM method, which can be implemented in real-time, and does not require conservative assumptions for integrity risk computation.

In Section II of this paper, a batch least-squares residual-based RAIM algorithm is presented. This batch approach is similar to the well-established snapshot RAIM, but it is applied to a sequence of measurements and system dynamics over a finite window in time. Least-squares batch implementations can be implemented sequentially using a sliding-window mechanism, but it requires considerable computation and memory resources for the storage and processing of past-time measurements and state coefficients – which is why we ultimately pursue a KF-based RAIM approach.

Still, in this work, the well-understood batch RAIM approach is used to derive results that will be extended to KF RAIM. For instance, given a time sequence of measurements and state dynamics, we can exploit the fact that the current-time state estimates are identical for a KF and for a batch. In addition, a batch is expressed in a single measurement equation and is much easier to analyze than a KF (which iteratively processes multiple equations). Finally and most importantly, batch RAIM is a direct extension of snapshot RAIM, which highlights two conditions that facilitate direct integrity risk computation: first, the state estimate and detection test statistic must be stochastically independent, and second, their probability distributions must be known. The KF RAIM test statistic is carefully designed to satisfy these two key-conditions.

Section III introduces a KF RAIM method that uses the weighted norm of the current-time KF residual as a detection test statistic. First, based on batch RAIM analysis, this test statistic is shown to be independent from the estimate error. Second, the current-time residual probability distribution is derived. The current-time test-statistic is proved to follow a generalized non-central chi-square distribution, whose parameters are fully identified and can be computed recursively. Thus, Section III describes a sequential RAIM algorithm that enables exact integrity risk evaluation. But a KF also generates past-time state estimates and residuals, which could be exploited to improve detection of faults that persist in time, and could provide early indicators of threats affecting current-time and future-time state estimates.

Therefore, in Section IV of this paper, a full KF RAIM method is introduced. First, current-time results derived in Section III are utilized to establish the probability distributions of past-time residuals. Second, a proof is given of statistical independence between current-time state estimates and past-time residuals. As a result, KF RAIM achieves rigorous integrity risk evaluation using a

test-statistic that is recursively updated (by simply adding a current-time component to an accumulated past-time-residual-based test statistic).

Finally, in Section V, the integrity monitoring performance of both batch RAIM and KF RAIM is illustrated for a benchmark application of aircraft precision approach. The two methods are evaluated against single-satellite fault profiles, for sequences of measurements collected over a fixed time-interval and for numerous satellite geometries. System availability is quantified for a multi-constellation carrier-phase based navigation system, at multiple locations over the Contiguous United States (CONUS).

II. BATCH RESIDUAL-BASED RAIM

The batch least squares residual-based RAIM algorithm (or batch RAIM) was derived in a previous paper as a direct extension of the well-established snapshot RAIM method [19]. It is basically presented here and is used in Sections III and IV to derive results relevant to the KF RAIM approach.

Linear Dynamic System Description

A linear dynamic system is described at any epoch k of a time-sequence (spanning from epoch 1 to the current epoch noted q), by a measurement equation and a process equation:

$$\mathbf{z}_k = \mathbf{H}_k \mathbf{x}_k + \mathbf{v}_k \tag{1}$$

$$\mathbf{x}_{k+1} = \mathbf{\Phi}_k \mathbf{x}_k + \mathbf{w}_k \tag{2}$$

where:

- k ranges from 1 to q
- $\mathbf{z}_k$ is the $n_k \times 1$ vector of measurements at epoch k
- $\mathbf{x}_k$ is the $m_k \times 1$ state vector
- $\mathbf{H}_k$ is the observation matrix
- $\mathbf{v}_k$ is the measurement noise vector
- $\mathbf{f}_k$ is the fault vector (to be detected)
- $\mathbf{\Phi}_k$ is the state propagation matrix
- $\mathbf{w}_k$ is the process noise vector.

Vector $\mathbf{v}_k$ is assumed normally distributed with zero mean and covariance matrix $\mathbf{V}_k$. We use the notation:

$$\mathbf{v}_k \sim \mathrm{N}(\mathbf{0}, \mathbf{V}_k).$$

We also assume that: $\mathbf{w}_k \sim \mathrm{N}(\mathbf{0}, \mathbf{W}_k)$.

Vectors $\mathbf{v}_k$ and $\mathbf{w}_k$ are assumed independent.

General Batch Realization

A general batch realization is obtained by simply stacking all measurement and process equations in a single batch measurement equation:

$$\mathbf{z}_Q = \mathbf{H}_Q \mathbf{x}_Q + \mathbf{v}_Q + \mathbf{f}_Q \tag{3}$$

where

$$\mathbf{z}_Q = \begin{bmatrix} \mathbf{z}_1^T & \mathbf{0} & \cdots & \mathbf{0} & \mathbf{z}_k^T & \mathbf{0} & \cdots & \mathbf{z}_q^T \end{bmatrix}^T$$

$$\mathbf{H}_Q = \begin{bmatrix} \mathbf{H}_1 & \mathbf{0} & \cdots & & & & & \mathbf{0} \\ \mathbf{\Phi}_1 & -\mathbf{I} & \cdots & & & & & \vdots \\ \vdots & & & & & & & \\ \mathbf{0} & \cdots & & \mathbf{\Phi}_{k-1} & -\mathbf{I} & \mathbf{0} & \cdots & \mathbf{0} \\ \mathbf{0} & \cdots & & \mathbf{0} & \mathbf{H}_k & \mathbf{0} & \cdots & \mathbf{0} \\ \mathbf{0} & \cdots & & \mathbf{0} & \mathbf{\Phi}_k & -\mathbf{I} & \cdots & \mathbf{0} \\ \vdots & & & & & & & \\ \mathbf{0} & \cdots & & & & \cdots & \mathbf{0} & \mathbf{H}_q \end{bmatrix}$$

$$\mathbf{x}_Q = \begin{bmatrix} \mathbf{x}_1^T & \mathbf{x}_2^T & \cdots & \mathbf{x}_{k-1}^T & \mathbf{x}_k^T & \mathbf{x}_{k+1}^T & \cdots & \mathbf{x}_q^T \end{bmatrix}^T$$

$$\mathbf{v}_Q = \begin{bmatrix} \mathbf{v}_1^T & \mathbf{w}_1^T & \cdots & \mathbf{w}_{k-1}^T & \mathbf{v}_k^T & \mathbf{w}_k^T & \cdots & \mathbf{v}_q^T \end{bmatrix}^T$$

$$\mathbf{f}_Q = \begin{bmatrix} \mathbf{f}_1^T & \mathbf{0} & \cdots & \mathbf{0} & \mathbf{f}_k^T & \mathbf{0} & \cdots & \mathbf{f}_q^T \end{bmatrix}^T$$

For any epoch k, the capital subscript K designates epochs 1 to k (i.e., for the current epoch q, Q designates all epochs during the time sequence). We respectively note n_Q and m_Q the total numbers of measurements and of states for the entire time interval.

It is worth noticing that the covariance matrix $\mathbf{V}_Q$ of the batch measurement noise vector $\mathbf{v}_Q$ is block diagonal, with block matrices:

$$\mathbf{V}_1, \quad \mathbf{W}_1, \quad \ldots, \quad \mathbf{W}_{k-1}, \quad \mathbf{V}_k, \quad \mathbf{W}_k, \quad \ldots, \quad \mathbf{V}_q$$

Despite $\mathbf{V}_Q$ being block-diagonal, measurement noise correlation can be incorporated by state augmentation [20] while preserving the general batch formulation of equation 3. Also, prior knowledge on state variables can be introduced by measurement augmentation (see [19] for example batch realizations).

Batch State Estimation

The batch least-squares state estimate vector $\hat{\mathbf{x}}_{Q|Q}$ of $\mathbf{x}_Q$ with covariance matrix $\mathbf{P}_{Q|Q}$ (the subscript '$Q|Q$' indicates an estimate of all states using all measurements), is given by:

$$\hat{\mathbf{x}}_{Q|Q} = \mathbf{S}_Q \mathbf{z}_Q \tag{4}$$

$$\mathbf{P}_{Q|Q} = \left(\mathbf{H}_Q^T \mathbf{V}_Q^{-1} \mathbf{H}_Q \right)^{-1} \tag{5}$$

where $\mathbf{S}_Q$ is the pseudo-inverse of the observation matrix $\mathbf{H}_Q$ weighted by $\mathbf{V}_Q^{-1}$:

$$\mathbf{S}_Q = \left(\mathbf{H}_Q^T \mathbf{V}_Q^{-1} \mathbf{H}_Q \right)^{-1} \mathbf{H}_Q^T \mathbf{V}_Q^{-1} \tag{6}$$

The state estimate error $\delta\mathbf{x}_{Q|Q}$ is defined as:

$$\delta \mathbf{x}_{Q|Q} \equiv \hat{\mathbf{x}}_{Q|Q} - \mathbf{x}_Q = \mathbf{S}_Q \left(\mathbf{v}_Q + \mathbf{f}_Q \right) \quad (7)$$

Navigation requirements often focus on a subset or on a linear combination of current-time states, noted $\delta x_{q|Q}$ (e.g., the emphasis is on the current-time vertical position coordinate for the example aircraft approach application investigated in Section V). The scalar $\delta x_{q|Q}$ can be expressed as:

$$\delta x_{q|Q} = \mathbf{T}_X^T \delta \mathbf{x}_{Q|Q} \quad (8)$$

where $\mathbf{T}_X$ is a $m_Q \times 1$ vector of state coefficients (e.g., a vector of zeros with a single one coefficient used to extract the current-time vertical position coordinate). We have:

$$\delta x_{q|Q} \sim \mathrm{N}(\mu_{q|Q} \ , \ \mathbf{T}_X^T \mathbf{P}_{Q|Q} \mathbf{T}_X) \quad (9)$$

where the mean $\mu_{q|Q}$ is a function of the fault profile $\mathbf{f}_Q$:

$$\mu_{q|Q} = \mathbf{T}_X^T \mathbf{S}_Q \mathbf{f}_Q \ . \quad (10)$$

Batch Fault Detection

Similar to the snapshot residual-based RAIM approach, a batch residual vector $\mathbf{r}_{Q|Q}$ is defined as:

$$\mathbf{r}_{Q|Q} \equiv \mathbf{z}_Q - \mathbf{H}_Q \hat{\mathbf{x}}_{Q|Q} \quad (11)$$

The norm of $\mathbf{r}_{Q|Q}$ weighted by $\mathbf{V}_Q^{-1}$ is the batch RAIM detection test statistic:

$$\left\| \mathbf{r}_{Q|Q} \right\|^2_{\mathbf{V}_Q^{-1}} = \mathbf{r}_{Q|Q}^T \mathbf{V}_Q^{-1} \mathbf{r}_{Q|Q} \quad (12)$$

From snapshot RAIM analysis [21], the test statistic $\left\| \mathbf{r}_{Q|Q} \right\|^2_{\mathbf{V}_Q^{-1}}$ is known to follow a non-central chi-square distribution with $n_Q - m_Q$ degrees of freedom and non-centrality parameter $\lambda^2_{Q|Q}$ (which is a function of the fault vector $\mathbf{f}_Q$). We use the notation:

$$\left\| \mathbf{r}_{Q|Q} \right\|^2_{\mathbf{V}_Q^{-1}} \sim \chi^2_{NC} \left(n_Q - m_Q, \ \lambda^2_{Q|Q} \right) \quad (13)$$

$$\lambda^2_{Q|Q} = \mathbf{f}_Q^T \mathbf{V}_Q^{-1} (\mathbf{I} - \mathbf{H}_Q \mathbf{S}_Q) \mathbf{f}_Q \quad (14)$$

where $\mathbf{I}$ is the identity matrix of appropriate dimensions.

Batch RAIM Integrity Risk Evaluation

Navigation integrity requirements are specified in terms of an alert limit AL, a continuity risk requirement P_C, and an integrity risk requirement $P_{HMI,REQ}$.

- Hazardous information is declared if the estimate error $\delta x_{q|Q}$ exceeds AL.
- The test statistic $\left\| \mathbf{r}_{Q|Q} \right\|^2_{\mathbf{V}_Q^{-1}}$ is evaluated against a threshold $T_{Q|Q}$, which is set in compliance with P_C to limit the probability of false alarms [21].

In the presence of a fault, the integrity risk or probability of hazardous misleading information P_{HMI} is defined as a joint probability:

$$P_{HMI} = P\left(\delta x_{q|Q} > AL, \ \left\| \mathbf{r}_{Q|Q} \right\|^2_{\mathbf{V}_Q^{-1}} < T_{Q|Q} \right) \quad (15)$$

Integrity risk evaluation is necessary to determine whether the integrity performance criterion is fulfilled, i.e., if the following equation is satisfied:

$$P_{HMI} < P_{HMI,REQ} / P_P \quad (16)$$

where P_P is the prior probability of fault occurrence.

From snapshot RAIM analysis, the random parts of $\delta x_{q|Q}$ and $\left\| \mathbf{r}_{Q|Q} \right\|^2_{\mathbf{V}_Q^{-1}}$ are proved to be statistically independent. [21] [22]. It follows from equation 15 that the integrity risk can be expressed as a product of probabilities:

$$P_{HMI} = P\left(\delta x_{q|Q} > AL \right) P\left(\left\| \mathbf{r}_{Q|Q} \right\|^2_{\mathbf{V}_Q^{-1}} < T_{Q|Q} \right) \quad (17)$$

In addition, both probability distributions of $\delta x_{q|Q}$ and $\left\| \mathbf{r}_{Q|Q} \right\|^2_{\mathbf{V}_Q^{-1}}$ are fully defined in equations 9 and 13. Therefore, the integrity risk of batch RAIM can be computed.

The above paragraphs explain that the two conditions:

- independence between state estimate and detection test statistic
- knowledge of their probability distributions

are instrumental when evaluating the integrity risk. In Sections III and IV, the KF RAIM test statistic will be carefully designed to satisfy these two key-conditions. But before tackling the KF RAIM algorithm, the batch RAIM residual is broken down into current and past-time components.

Partitioning the Batch: Equivalent Forward-Backward Smoother Formulation

As a transitional step towards deriving a KF RAIM algorithm, we consider a RAIM method based on a forward-backward smoother, which is equivalent to a batch, but is computationally more efficient (see [23] for additional details).

The batch RAIM residual is partitioned into individual residual components at each epoch, for the measurement and for the process equations. Each individual component can be expressed using the batch residual definition in equation 11 (and the definition of the sparse batch observation matrix $\mathbf{H}_Q$ in equation 3):

$$\mathbf{r}_{Q|Q} = \begin{bmatrix} \mathbf{r}_{1|Q} \\ \mathbf{r}_{W,1|Q} \\ \vdots \\ \mathbf{r}_{k|Q} \\ \mathbf{r}_{W,k|Q} \\ \vdots \\ \mathbf{r}_{q|Q} \end{bmatrix} = \begin{bmatrix} \mathbf{z}_1 - \mathbf{H}_1\hat{\mathbf{x}}_{1|Q} \\ -\boldsymbol{\Phi}_1\hat{\mathbf{x}}_{1|Q} + \hat{\mathbf{x}}_{2|Q} \\ \vdots \\ \mathbf{z}_k - \mathbf{H}_k\hat{\mathbf{x}}_{k|Q} \\ -\boldsymbol{\Phi}_k\hat{\mathbf{x}}_{k|Q} + \hat{\mathbf{x}}_{k+1|Q} \\ \vdots \\ \mathbf{z}_q - \mathbf{H}_q\hat{\mathbf{x}}_{q|Q} \end{bmatrix} \quad (18)$$

It turns out that individual residual components have simple expressions. For example, the current-time residual component $\mathbf{r}_{q|Q}$ is expressed in terms of the current-time measurement and state estimate vectors ($\mathbf{z}_q$ and $\hat{\mathbf{x}}_{q|Q}$). It can be computed at the q^{th} forward filter iteration (i.e., at the current-time iteration of the Kalman filter). Also, each preceding residual component in $\mathbf{r}_{Q|Q}$ can be recovered while smoothing the data backwards.

In addition, we emphasized the fact that the batch measurement noise covariance matrix $\mathbf{V}_Q$ was block-diagonal. It follows that the weighted norm squared of the batch residual in equation 12 can be expressed as a sum of squares of weighted norms:

$$\left\|\mathbf{r}_{Q|Q}\right\|^2_{\mathbf{V}_Q^{-1}} = \sum_{k=1}^{q}\left\|\mathbf{r}_{k|Q}\right\|^2_{\mathbf{V}_k^{-1}} + \sum_{k=1}^{q-1}\left\|\mathbf{r}_{W,k|Q}\right\|^2_{\mathbf{W}_k^{-1}} \quad (19)$$

Each term of the sum corresponds to an individual residual component expressed in equation 18, and it is weighted by it corresponding block matrix in $\mathbf{V}_Q^{-1}$.

Particularly relevant in this work is the fact that the current-time batch residual component $\mathbf{r}_{q|Q}$ and its weighted norm can be computed using a KF. We use this observation as a starting point to derive the KF-based RAIM method.

III. CURRENT-TIME KF RESIDUAL

The current time state estimate vector $\hat{\mathbf{x}}_{q|Q}$ and residual component $\mathbf{r}_{q|Q}$ are identical for the batch and for the KF. It is not the case at past-time epochs, where the KF state estimate vector $\hat{\mathbf{x}}_{k|K}$ differs from the batch estimate $\hat{\mathbf{x}}_{k|Q}$. In a first stage of the KF RAIM design, the weighted norm of $\mathbf{r}_{q|Q}$, which is defined as:

$$\left\|\mathbf{r}_{q|Q}\right\|^2_{\mathbf{V}_q^{-1}} = \mathbf{r}_{q|Q}^T\mathbf{V}_q^{-1}\mathbf{r}_{q|Q} \quad (20)$$

is used as a detection test statistic. The following paragraphs address the two key-conditions that $\left\|\mathbf{r}_{q|Q}\right\|^2_{\mathbf{V}_q^{-1}}$ should satisfy to enable integrity risk evaluation.

First, the current-time KF residual vector component $\mathbf{r}_{q|Q}$ in equation 18 can be expressed as a function of the batch residual vector $\mathbf{r}_{Q|Q}$ (known to lay in the parity space – or left null space – of $\mathbf{H}_Q$ [22]):

$$\mathbf{r}_{q|Q} = \begin{bmatrix}\mathbf{0} & \mathbf{I}\end{bmatrix}\mathbf{r}_{Q|Q} \quad (21)$$

It means that the vector $\mathbf{r}_{q|Q}$ is included in a subspace of the parity space of matrix $\mathbf{H}_Q$. On the other hand, $\hat{\mathbf{x}}_{q|Q}$ is derived from components of $\mathbf{z}_Q$ that belong to the range of $\mathbf{H}_Q$ (i.e., to the column space of $\mathbf{H}_Q$, which is the orthogonal complement of its left null space). Therefore, $\mathbf{r}_{q|Q}$ is statistically independent from $\hat{\mathbf{x}}_{q|Q}$ so that the integrity risk can be expressed as a product of probabilities:

$$P_{HMI} = P\left(\delta x_{q|Q} > AL\right)P\left(\left\|\mathbf{r}_{q|Q}\right\|^2_{\mathbf{V}_q^{-1}} < T_{q|Q}\right) \quad (22)$$

Second, the probability distribution of $\delta x_{q|Q}$ is given in equation 9 (the distribution of $\delta x_{q|Q}$ is the same throughout the paper and does not need to be further mentioned). However, the probability distribution of $\left\|\mathbf{r}_{q|Q}\right\|^2_{\mathbf{V}_q^{-1}}$ is unknown. Notice in equation 19 that the distribution of the total sum of partial test statistics is fully defined (in equation 13), but the distribution of individual terms of the sum is undetermined.

Theorem 1: Probability Distribution of the Current-Time Test Statistic

The current-time test statistic follows a *generalized non-central chi-square* distribution (proof in Appendix I). Indeed, the current-time test statistic can be expressed as a weighted sum of independent non-central chi-square distributed random variables:

$$\left\|\mathbf{r}_{q|Q}\right\|^2_{\mathbf{V}_q^{-1}} = \sum_{i=1}^{p}\alpha_i^2 y_i^2 \quad (23)$$

where the weights α_i and the independent, identically distributed (i.i.d.) variables y_i can be determined by singular value decomposition (SVD) of matrix $\mathbf{A}$:

$$\mathbf{A} = \mathbf{V}_q^{-1/2}\begin{bmatrix}\mathbf{0} & \mathbf{I}\end{bmatrix}\left(\mathbf{I} - \mathbf{H}_Q\mathbf{S}_Q\right)\mathbf{V}_Q^{1/2} \quad (24)$$

The SVD is noted: $\mathbf{A} = \mathbf{U}_L\boldsymbol{\Lambda}\mathbf{U}_R^T$.

The coefficients α_i are the non-zero singular values of $\mathbf{A}$ (non-zero elements of the diagonal matrix $\boldsymbol{\Lambda}$, and

$$y_i \sim \mathrm{N}\left(\begin{bmatrix}\mathbf{0} & \alpha_i^{-1} & \mathbf{0}\end{bmatrix}\mathbf{U}_L^T\mathbf{V}_q^{-1/2}\mathbf{r}_{q|Q},\ 1\right).$$

Equation 23 defines a generalized non-central chi-square distribution. It can not be expressed analytically without an integral form or an infinite sum [24], but its cumulative distribution function (CDF) can be computed numerically

to any desired level of accuracy using published algorithms (we use reference [25]).

Theorem 1 expresses the probability distribution of a partial test-statistic in terms of batch matrices (subscript Q in equation 24). This is not practical for sequential implementations.

Corollary to Theorem 1: Distribution of the Current-Time Test Statistic for Recursive Implementation

The current-time test statistic can be expressed as (proof in Appendix II):

$$\left\|\mathbf{r}_{q|Q}\right\|^2_{\mathbf{V}_q^{-1}} = \sum_{i=1}^{p_B} \alpha_{B,i}^2 y_{B,i}^2 \tag{25}$$

where $\alpha_{B,i}$ are non-zero singular values of $\mathbf{B}$,

$$\mathbf{B} = \mathbf{V}_q^{-1/2}\mathbf{M} = \mathbf{U}_{LB}\mathbf{\Lambda}_B\mathbf{U}_{RB}^T \tag{26}$$

and $\quad y_{B,i} \sim \mathrm{N}\left(\begin{bmatrix}\mathbf{0} & \alpha_{B,i}^{-1} & \mathbf{0}\end{bmatrix}\mathbf{U}_{LB}^T\mathbf{V}_q^{-1/2}\mathbf{r}_{q|Q}\ ,\ 1\right)$

The matrix $\mathbf{M}$ is expressed in terms of the current-time KF gain $\mathbf{K}_q$, and of the KF state covariance matrix $\mathbf{P}_{q-1|Q-1}$ at the preceding epoch:

$$\mathbf{M} = \begin{bmatrix}\left(\mathbf{I}-\mathbf{H}_q\mathbf{K}_q\right)\mathbf{V}_q^{1/2} & -\mathbf{H}_q\left(\mathbf{I}-\mathbf{K}_q\mathbf{H}_q\right)\mathbf{\Phi}_{q-1}\mathbf{P}_{q-1|Q-1}^{1/2}\end{bmatrix}.$$

Section III has proved that the weighted norm of the current-time residual can be used as an easy-to-compute test statistic (equation 20) for sequential fault-detection, and that it enables direct integrity risk evaluation. Section IV will show that past-time residuals can also be exploited, which will improve the detection of faults that last in time, and will provide early indicators of faults affecting current-time state estimates.

IV. KALMAN FILTER-BASED RAIM

Unlike current-time state estimates and residual vectors, past-time components for the KF ($\hat{\mathbf{x}}_{k|K}$ and $\mathbf{r}_{k|K}$) differ from the batch components ($\hat{\mathbf{x}}_{k|Q}$ and $\mathbf{r}_{k|Q}$). In response, at any past-time epoch *k*, we consider a *truncated* batch measurement equation, represented in Fig. 1 as a partition of the entire batch, and expressed as:

$$\mathbf{z}_K = \mathbf{H}_K\mathbf{x}_K + \mathbf{v}_K + \mathbf{f}_K \tag{27}$$

In this case, the state estimate vector $\hat{\mathbf{x}}_{k|K}$ at epoch *k* is the same for the KF as for the truncated batch. And the results that were established at the last epoch of the full batch are valid at the last epoch of the truncated batch. For example, the partial residual component at epoch *k* is given by:

$$\mathbf{r}_{k|K} = \mathbf{z}_k - \mathbf{H}_k\hat{\mathbf{x}}_{k|K} \tag{28}$$

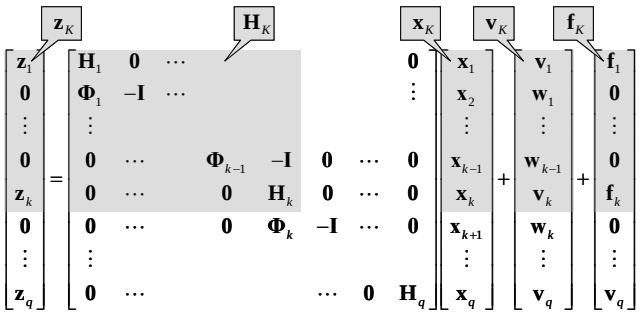

Fig. 1 Full Batch and Truncated Batch Realizations

Also, the weighted norm of the residual is:

$$\left\|\mathbf{r}_{k|K}\right\|^2_{\mathbf{V}_k^{-1}} = \mathbf{r}_{k|K}^T\mathbf{V}_k^{-1}\mathbf{r}_{k|K} \tag{29}$$

which can easily be computed at epoch *k* using a KF. One can briefly note that unlike for the batch, the residual contribution corresponding to KF state predictions is null:

$$\mathbf{r}_{W,k|K} = -\mathbf{\Phi}_k\hat{\mathbf{x}}_{k|K} + \hat{\mathbf{x}}_{k+1|K} = \mathbf{0} \tag{30}$$

The next paragraphs will show that $\left\|\mathbf{r}_{k|K}\right\|^2_{\mathbf{V}_k^{-1}}$ satisfies the two key-conditions mentioned in Section I.

First, the probability distribution of the partial residual's weighted norm $\left\|\mathbf{r}_{k|K}\right\|^2_{\mathbf{V}_k^{-1}}$ is determined using Theorem 1 and its Corollary. Theorem 1 can be derived using the truncated batch instead of the full batch (in Appendix I). Proof for the Corollary for past-time residuals directly follows from equation 28 (see Appendix II). It follows that both Theorem 1 and its Corollary remain valid when replacing current-time subscripts *q* and *Q* with past-time indices *k* and *K*.

Second, independence between the current-time state estimate $\delta x_{q|Q}$ and past-time KF residuals $\mathbf{r}_{k|K}$ is established in Theorem 2.

Theorem 2: Statistical Independence between Current-Time State Estimates and Past-Time Test-Statistics

The random parts of the current-time state estimate vector $\hat{\mathbf{x}}_{q|Q}$ and of the past-time KF residual vector component $\mathbf{r}_{k|K}$ (at any epoch *k* of the filtering interval) are derived from orthogonal components of the batch measurement noise vector $\mathbf{v}_Q$ (proof in Appendix III).

This means that both current and past-time residual components can contribute to the KF RAIM test statistic because they satisfy the two key-conditions that enable integrity risk computation.

Summary of the Kalman Filter RAIM Method

The full KF RAIM test statistic is a sum of weighted norms squared including current and past-time residual contributions:

$$\left\|\mathbf{r}_{KF,Q}\right\|^2_{\mathbf{V}_Q^{-1}} = \sum_{k=1}^{q}\left\|\mathbf{r}_{k|K}\right\|^2_{\mathbf{V}_{V,k}^{-1}} \qquad (31)$$

It is easily, recursively updated by adding the current-time component to the previously computed test-statistic.

The KF RAIM test statistic is a sum of generalized non-central chi-squared random variables, whose parameters are identified in Theorem 1 and can be computed recursively using the Corollary. In Theorem 2, $\left\|\mathbf{r}_{KF,Q}\right\|^2_{\mathbf{V}_Q^{-1}}$ is shown to be statistically independent from the estimate error, so that the integrity can be evaluated as:

$$P_{HMI} = P\left(\delta x_{q|Q} > AL\right)P\left(\left\|\mathbf{r}_{KF,Q}\right\|^2_{\mathbf{V}_Q^{-1}} < T_{KF}\right) \qquad (32)$$

For practical implementations, a step-by-step formulation of the KF RAIM method is given below:

- using the previously derived state estimate vector $\hat{\mathbf{x}}_{q-1|Q-1}$ and a KF test statistic $\left\|\mathbf{r}_{KF,Q-1}\right\|^2_{\mathbf{V}_{Q-1}^{-1}}$, compute $\hat{\mathbf{x}}_{q|Q}$ and $\left\|\mathbf{r}_{q|Q}\right\|^2_{\mathbf{V}_q^{-1}}$, which are used to obtain $\left\|\mathbf{r}_{KF,Q}\right\|^2_{\mathbf{V}_Q^{-1}}$
- determine the probability distribution of $\left\|\mathbf{r}_{KF,Q}\right\|^2_{\mathbf{V}_Q^{-1}}$ using the Corollary to Theorem 1
- compute the detection threshold T_{KF} (using the inverse CDF of the previously defined generalized chi-square distribution – under fault-free conditions)
- if $\left\|\mathbf{r}_{KF,Q}\right\|^2_{\mathbf{V}_Q^{-1}} > T_{KF}$, a fault was successfully detected; in the other case, evaluate the integrity risk (using the CDF of the previously defined generalized non-central chi-square distribution, now under faulted conditions) to determine current-time availability

V. PERFORMANCE ANALYSIS

Availability Analysis for Aircraft Precision Approach

The performance analysis is structured around the benchmark application of aircraft precision approach, where an airplane flies toward a runway at a constant 70 m/s velocity, along a constant 3 deg glide slope angle. GPS and Galileo ranging observations collected over a 10 min time period are used in the estimation and detection algorithms. To account for various satellite geometries, approaches starting at regular 4 min intervals are considered over a 24 hour period. The percentage of approaches that meets the integrity performance criterion (equation 16) over the total number of simulated approaches is the measure of fault-detection performance or RAIM availability.

It is further assumed that the user has real-time access to measurements from a nearby reference station. At each epoch k, ionospheric-error-free differential code $\boldsymbol{\rho}_k$ and carrier phase $\boldsymbol{\varphi}_k$ measurements for all satellites are stacked together in a measurement vector:

$$\begin{bmatrix}\boldsymbol{\rho}\\ \boldsymbol{\varphi}\end{bmatrix}_k = \begin{bmatrix}\mathbf{G}_k & 1 & \mathbf{0} & \mathbf{H}_{ERR,\rho,k}\\ \mathbf{G}_k & 1 & \mathbf{I}_{n_k} & \mathbf{H}_{ERR,\phi,k}\end{bmatrix}\begin{bmatrix}\mathbf{x}_{U,k}\\ \tau_k\\ \mathbf{n}\\ \mathbf{s}_{ERR,k}\end{bmatrix} + \begin{bmatrix}\mathbf{v}_\rho\\ \mathbf{v}_\phi\end{bmatrix}_k \qquad (33)$$

where

- $\mathbf{G}_k$ is the satellite geometry matrix
- $\mathbf{x}_{U,k}$ is the user position (in a local reference frame, with respect to the reference station location),
- τ_k is the differential receiver clock bias
- $\mathbf{n}$ is the vector of differenced cycle ambiguities

The single-difference iono-free code and carrier phase measurement multipath and receiver noise vectors are respectively defined as:

$$\mathbf{v}_{\rho,k} \sim \mathrm{N}\left(\mathbf{0},\, \mathbf{I}\sigma_\rho^2\right) \quad \text{and} \quad \mathbf{v}_{\phi,k} \sim \mathrm{N}\left(\mathbf{0},\, \mathbf{I}\sigma_\phi^2\right)$$

An inflation factor accounts for the differential iono-free measurement combination (refer to [19] for details). In addition, a vector of error states $\mathbf{s}_{ERR}$ is included in the state vector to incorporate the dynamics of the error sources (matrix $\mathbf{H}_{ERR}$ contains the corresponding state coefficients). In this work, error sources other than $\mathbf{v}_{\rho,k}$ and $\mathbf{v}_{\phi,k}$ include satellite orbit ephemeris errors and horizontal tropospheric decorrelation, both modeled as constant gradients (over time and over change in aircraft altitude, respectively). We use the measurement error model parameter values employed in [19], for single differenced iono-free measurements (we remove the satellite clock error and the residual orbit ephemeris and tropospheric biases). Samples are taken at infrequent two-minute intervals where measurements are assumed to be uncorrelated.

The process equation accounts for various types of dynamics:

$$\begin{bmatrix} \mathbf{x}_{U,k+1} \\ \tau_{k+1} \\ \mathbf{n} \\ \mathbf{s}_{ERR,k+1} \end{bmatrix} = \begin{bmatrix} \mathbf{0} & \mathbf{0} & \mathbf{0} & \mathbf{0} \\ \mathbf{0} & 0 & \ddots & \vdots \\ \vdots & \ddots & \mathbf{I} & \mathbf{0} \\ \mathbf{0} & \cdots & \mathbf{0} & \mathbf{\Phi}_{ERR,k} \end{bmatrix} \begin{bmatrix} \mathbf{x}_{U,k} \\ \tau_k \\ \mathbf{n} \\ \mathbf{s}_{ERR,k} \end{bmatrix} + \begin{bmatrix} \mathbf{w}_U \\ \mathbf{w}_T \\ \mathbf{0} \\ \mathbf{w}_{ERR} \end{bmatrix}_k \quad (34)$$

Equation 34 includes states whose time propagation is unknown ($\mathbf{x}_{U,k}$ and τ_k) and for which the zero-mean normally-distributed process noise ($\mathbf{w}_U$ and $\mathbf{w}_T$) has a very large standard deviation. In this preliminary analysis, the state vector components $\mathbf{n}$ and $\mathbf{s}_{ERR}$ are assumed constant (i.e., $\mathbf{\Phi}_{ERR} = \mathbf{I}$ and $\mathbf{w}_{ERR} = \mathbf{0}$). Prior knowledge on $\mathbf{s}_{ERR}$ is introduced at filter initiation [19], whereas $\mathbf{n}$ is initially unknown.

The threat model (or assumed fault vector, not expressed in equation 33) is composed of worst-case single-satellite measurement fault profiles, which maximize the integrity of batch RAIM (a detailed derivation of these fault modes in given in reference [26]). .

Navigation requirements include an aggressive vertical alert limit or VAL of 8 m (which will generate performance variations), a continuity risk requirement P_C of $8 \cdot 10^{-6}$ and an integrity requirement $P_{HMI,REQ}$ of 10^{-7}. We assume a prior probability of fault P_P of $2.5 \cdot 10^{-5}$ (failure rate of 10^{-4}/hr over 15min exposure periods).

Performance Comparison between Batch and KF RAIM Methods over CONUS

The performance of the batch and KF RAIM methods is analyzed for a $5\text{deg} \times 7.5\text{deg}$ latitude-longitude grid of locations over CONUS. The same sequence of measurements and the same fault profiles are used for both algorithms.

Fig. 2 and 3 presents availability maps for the batch RAIM and KF RAIM methods, respectively. RAIM availability is color-coded: white color corresponds to 100%, black corresponds to 70% (constant availability contours are also plotted). The batch RAIM method performs slightly better than the KF procedure, but in both cases availability ranges approximately between 97% and 100%. Higher batch RAIM availability is to be expected because the sensitivity of past-time batch residuals (computed using $\hat{\mathbf{x}}_{k|Q}$ in equation 18) is higher than that of past-time KF residuals (derived from $\hat{\mathbf{x}}_{k|K}$). Still, for this example application, the availability results obtained using a computation and memory-intensive batch RAIM method are almost identical to the ones generated by this new recursive KF RAIM algorithm.

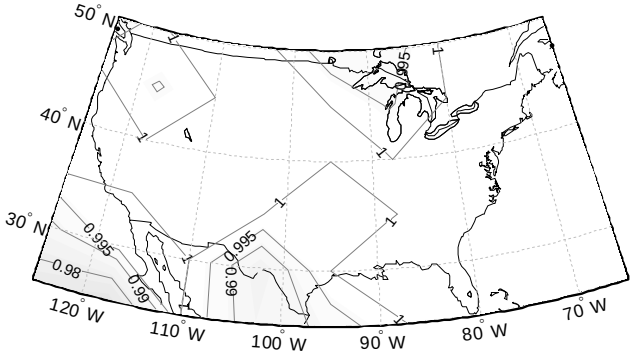

Fig. 2 Availability Map for Batch RAIM

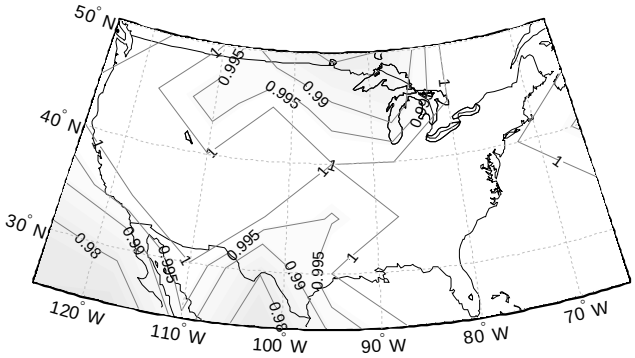

Fig. 3 Availability Map for KF RAIM

Fig. 4 displays the availability map of a KF RAIM approach that only uses the current-time test statistic (as suggested in Section III). In this case, availability drops to 72% at a few locations (versus 97% for the full KF RAIM method). Fig. 4 emphasizes the benefit of using both current and past-time measurements, which is made possible using the KF RAIM approach derived in Section IV.

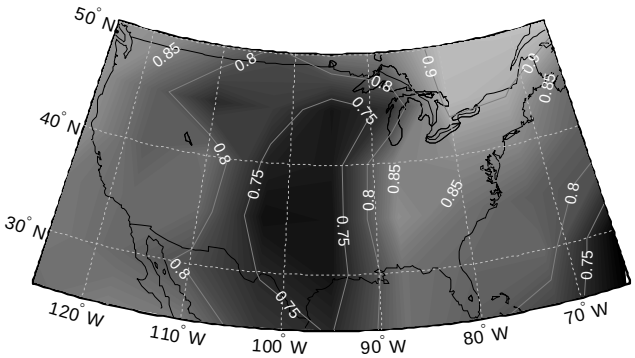

Fig. 4 Availability Map Using Only the Current-Time KF RAIM Residual

VI. CONCLUSION

This paper introduced a new Kalman filter-based RAIM method for navigation systems that require measurement filtering over time. The recursively-updated KF RAIM test statistic was specifically designed to exploit both current-time and past-time residual contributions while satisfying two key-conditions. First, it was proved to be statistically independent from the current-time state estimate error. Second, it was derived as sum of generalized non-central chi-square distributed variables. As a result, the easy-to-implement KF RAIM algorithm enables direct and rigorous integrity risk evaluation. Availability analyses were carried out for an example aircraft navigation application where differential GNSS carrier phase signals were used for positioning. Results showed that the new recursive method could achieve a level of performance similar to that of a much more computationally and memory-expensive batch RAIM procedure. The KF RAIM method opens the possibility for efficient, real-time KF-based navigation with the assurance of an accurate (i.e., not overly-conservative) integrity risk estimate.

APPENDIX I. PROOF OF THEOREM 1

Theorem 1: Probability Distribution of the Current-Time Test Statistic

The current-time component of the batch residual vector can be expressed using the definitions of equations 4, 11 and 18 as:

$$\mathbf{r}_{q|Q} = \begin{bmatrix}\mathbf{0} & \mathbf{I}\end{bmatrix}\left(\mathbf{I} - \mathbf{H}_Q\mathbf{S}_Q\right)\mathbf{z}_Q . \tag{35}$$

The first step of the proof is to normalize the measurement vector $\mathbf{z}_Q$. Consider the change of variable

$$\mathbf{z}_{Q^*} = \mathbf{V}_Q^{-1/2}\mathbf{z}_Q \quad , \quad \mathbf{z}_{Q^*} \sim \mathrm{N}\left(\mathbf{V}_Q^{-1/2}\mathbf{f}_Q \ , \ \mathbf{I}\right) \tag{36}$$

The vector $\mathbf{z}_{Q^*}$ of independent, identically distributed (i.i.d.) variables is substituted back into equation 35

$$\mathbf{r}_{q|Q} = \begin{bmatrix}\mathbf{0} & \mathbf{I}\end{bmatrix}\left(\mathbf{I} - \mathbf{H}_Q\mathbf{S}_Q\right)\mathbf{V}_Q^{1/2}\mathbf{z}_{Q^*} . \tag{37}$$

The weighted norm of $\mathbf{r}_{q|Q}$ defined in equation 20 can be expressed as a quadratic form of i.i.d. Gaussian random variables:

$$\left\|\mathbf{r}_{q|Q}\right\|^2_{\mathbf{V}_q^{-1}} = \mathbf{z}_{Q^*}^T\mathbf{A}^T\mathbf{A}\mathbf{z}_{Q^*} \tag{38}$$

where $$\mathbf{A} = \mathbf{V}_q^{-1/2}\begin{bmatrix}\mathbf{0} & \mathbf{I}\end{bmatrix}\left(\mathbf{I} - \mathbf{H}_Q\mathbf{S}_Q\right)\mathbf{V}_Q^{1/2} \tag{39}$$

The singular value decomposition (SVD) of $\mathbf{A}$ is noted:

$$\mathbf{A} = \mathbf{U}_L\mathbf{\Lambda}\mathbf{U}_R^T \tag{40}$$

Substituting equation 40 into 38 and simplifying yields:

$$\left\|\mathbf{r}_{q|Q}\right\|^2_{\mathbf{V}_q^{-1}} = \mathbf{z}_{Q^*}^T\mathbf{U}_R\mathbf{\Lambda}^2\mathbf{U}_R^T\mathbf{z}_{Q^*} \tag{41}$$

We use a second change of variable to recover a known quadratic form:

$$\mathbf{y} = \mathbf{U}_R^T\mathbf{z}_{Q^*} \quad , \quad \mathbf{y} \sim \mathrm{N}\left(\mathbf{U}_R^T\mathbf{V}_Q^{-1/2}\mathbf{f}_Q \ , \ \mathbf{I}\right) \tag{42}$$

$$\left\|\mathbf{r}_{q|Q}\right\|^2_{\mathbf{V}_q^{-1}} = \mathbf{y}^T\mathbf{\Lambda}^2\,\mathbf{y} \tag{43}$$

which is equivalent to equation 23:

$$\left\|\mathbf{r}_{q|Q}\right\|^2_{\mathbf{V}_q^{-1}} = \sum_{i=1}^{p}\alpha_i^2 y_i^2$$

where the α_i coefficients are the singular values of $\mathbf{A}$. The independent random variables y_i are expressed in equation 42 in terms of $\mathbf{f}_Q$, which is unknown in practice.

The following paragraph expresses $\mathbf{y}$ in terms of $\mathbf{r}_{q|Q}$. Equation 20 is first rewritten as:

$$\left\|\mathbf{r}_{q|Q}\right\|^2_{\mathbf{V}_q^{-1}} = \mathbf{r}_{q|Q}^T\mathbf{V}_q^{-1/2}\mathbf{V}_q^{-1/2}\mathbf{r}_{q|Q} \tag{44}$$

Then, substituting equation 40 and 42 into 38 and then back into equation 44 produces:

$$\mathbf{r}_{q|Q}^T\mathbf{V}_q^{-1/2}\mathbf{V}_q^{-1/2}\mathbf{r}_{q|Q} = \mathbf{y}^T\mathbf{\Lambda}\mathbf{U}_L^T\mathbf{U}_L\mathbf{\Lambda}\mathbf{y} \tag{45}$$

Therefore, $$\mathbf{V}_q^{-1/2}\mathbf{r}_{q|Q} = \mathbf{U}_L\mathbf{\Lambda}\mathbf{y} \tag{46}$$

Finally, for each non-zero element α_i of the diagonal matrix $\mathbf{\Lambda}$, the i.i.d. y_i variables can be isolated and their distribution is expressed as:

$$y_i \sim \mathrm{N}\left(\begin{bmatrix}\mathbf{0} & \alpha_i^{-1} & \mathbf{0}\end{bmatrix}\mathbf{U}_L^T\mathbf{V}_q^{-1/2}\mathbf{r}_{q|Q} \ , \ 1\right) \tag{47}$$

This concludes the proof of Theorem 1.

APPENDIX II. PROOF OF COROLLARY TO THEOREM 1

Corollary to Theorem 1: Distribution of the Current-Time Test Statistic for Recursive Implementation

The corollary to Theorem 1 aims at expressing the probability distribution of $\left\|\mathbf{r}_{q|Q}\right\|^2_{\mathbf{V}_q^{-1}}$ without using batch notations as in equation 24.

Consider the KF time update and measurement update equations:

$$\hat{\mathbf{x}}_{q-1|Q} = \mathbf{\Phi}_{q-1}\hat{\mathbf{x}}_{q-1|Q-1} \tag{48}$$

$$\hat{\mathbf{x}}_{q|Q} = \hat{\mathbf{x}}_{q-1|Q} + \mathbf{K}_q\left(\mathbf{z}_q - \mathbf{H}_q\hat{\mathbf{x}}_{q-1|Q}\right) \tag{49}$$

These two equations are combined in a single equation:

$$\hat{\mathbf{x}}_{q|Q} = \mathbf{K}_q\mathbf{z}_q + \left(\mathbf{I} - \mathbf{K}_q\mathbf{H}_q\right)\mathbf{\Phi}_{q-1}\hat{\mathbf{x}}_{q-1|Q-1} \tag{50}$$

The right-hand-side terms in equation 50 were rearranged to isolate the random vectors $\mathbf{z}_q$ and $\hat{\mathbf{x}}_{q-1|Q-1}$, which are statistically independent from each other.

Equation 18 established that:

$$\mathbf{r}_{q|Q} = \mathbf{z}_q - \mathbf{H}_q\hat{\mathbf{x}}_{q|Q} \tag{51}$$

Equation 50 is then substituted into 51:

$$\mathbf{r}_{q|Q} = \begin{bmatrix} \left(\mathbf{I} - \mathbf{H}_q \mathbf{K}_q\right) & -\mathbf{H}_q \left(\mathbf{I} - \mathbf{K}_q \mathbf{H}_q\right) \mathbf{\Phi}_{q-1} \end{bmatrix} \begin{bmatrix} \mathbf{z}_q \\ \hat{\mathbf{x}}_{q-1|Q-1} \end{bmatrix} \quad (52)$$

The remainder of the derivation is similar to Appendix I. We use a first change of variable:

$$\boldsymbol{\zeta} = \begin{bmatrix} \mathbf{V}_q^{-1/2} \mathbf{z}_q \\ \mathbf{P}_{q-1|Q-1}^{-1/2} \hat{\mathbf{x}}_{q-1|Q-1} \end{bmatrix} \quad , \quad \boldsymbol{\zeta} \sim \mathrm{N}\left(\begin{bmatrix} \mathbf{V}_q^{-1/2} \mathbf{f}_q \\ \mathbf{P}_{q-1|Q-1}^{-1/2} \boldsymbol{\mu}_{q-1|Q-1} \end{bmatrix} , \mathbf{I} \right)$$

where $\boldsymbol{\mu}_{q-1|Q-1}$ is the mean of $\hat{\mathbf{x}}_{q-1|Q-1}$. $\boldsymbol{\zeta}$ is a vector of i.i.d. random variables. We also note:

$$\mathbf{M} = \begin{bmatrix} \left(\mathbf{I} - \mathbf{H}_q \mathbf{K}_q\right) \mathbf{V}_q^{1/2} & -\mathbf{H}_q \left(\mathbf{I} - \mathbf{K}_q \mathbf{H}_q\right) \mathbf{\Phi}_{q-1} \mathbf{P}_{q-1|Q-1}^{1/2} \end{bmatrix}$$

hence,

$$\mathbf{r}_{q|Q} = \mathbf{M} \boldsymbol{\zeta} \quad (53)$$

The weighted norm of the residual is again expressed as a familiar quadratic form. By substituting equation 53 into 20, we can write:

$$\left\| \mathbf{r}_{q|Q} \right\|_{\mathbf{V}_q^{-1}}^2 = \boldsymbol{\zeta}^T \mathbf{B}^T \mathbf{B} \, \boldsymbol{\zeta} \quad (54)$$

where

$$\mathbf{B} = \mathbf{V}_q^{-1/2} \mathbf{M} \quad (55)$$

The SVD of $\mathbf{B}$ is noted:

$$\mathbf{B} = \mathbf{U}_{LB} \mathbf{\Lambda}_B \mathbf{U}_{RB}^T \quad (56)$$

which, substituted back into equation 54, yields:

$$\left\| \mathbf{r}_{q|Q} \right\|_{\mathbf{V}_q^{-1}}^2 = \boldsymbol{\zeta}^T \mathbf{U}_{RB} \mathbf{\Lambda}_B^2 \mathbf{U}_{RB}^T \boldsymbol{\zeta} \quad (57)$$

The second change of variable is:

$$\mathbf{y}_B = \mathbf{U}_{RB}^T \boldsymbol{\zeta} \quad , \quad \mathbf{y}_B \sim \mathrm{N}\left(\mathbf{U}_{RB}^T \begin{bmatrix} \mathbf{V}_q^{-1/2} \mathbf{f}_q \\ \mathbf{P}_{q-1|Q-1}^{-1/2} \boldsymbol{\mu}_{q-1|Q-1} \end{bmatrix} , \mathbf{I} \right) \quad (58)$$

Back to equation 57, we obtain:

$$\left\| \mathbf{r}_{q|Q} \right\|_{\mathbf{V}_q^{-1}}^2 = \mathbf{y}_B^T \mathbf{\Lambda}_B^2 \mathbf{y}_B \quad (58)$$

which is equivalent to equation 25:

$$\left\| \mathbf{r}_{q|Q} \right\|_{\mathbf{V}_q^{-1}}^2 = \sum_{i=1}^{p} \alpha_{B,i}^2 y_{B,i}^2 .$$

Finally, we can again express the distribution of $y_{B,i}^2$ variables in terms of $\mathbf{r}_{q|Q}$ following the exact same derivation as in the last paragraph of Appendix I, where $\mathbf{y}$, $\mathbf{U}_L$, $\mathbf{\Lambda}$, y_i and α_i are respectively replaced by $\mathbf{y}_B$, $\mathbf{U}_{LB}$, $\mathbf{\Lambda}_B$, $y_{B,i}$ and $\alpha_{B,i}$. This concludes the proof of the Corollary to Theorem 1.

APPENDIX III. PROOF OF THEOREM 2

Theorem 2: Statistical Independence between Current-Time State Estimates and Past-Time Test-Statistics

For the purpose of this derivation, we consider the fault-free batch measurement equation:

$$\mathbf{z}_Q = \mathbf{H}_Q \mathbf{x}_Q + \mathbf{v}_Q \quad (59)$$

The fault vector $\mathbf{f}_Q$ in equation 3 is left aside because deterministic parts of the measurement error do not affect the determination of statistical independence.

As in Appendices I and II, we use a change of variable to normalize the measurement equation:

$$\mathbf{z}_{Q^*} = \mathbf{H}_{Q^*} \mathbf{x}_Q + \delta \mathbf{z}_Q \quad (60)$$

where:

$$\mathbf{z}_{Q^*} = \mathbf{V}_Q^{-1/2} \mathbf{z}_Q \quad (61)$$

$$\mathbf{H}_{Q^*} = \mathbf{V}_Q^{-1/2} \mathbf{H}_Q \quad \text{and} \quad \delta \mathbf{z}_Q = \mathbf{V}_Q^{-1/2} \mathbf{v}_Q$$

We have: $\delta \mathbf{z}_Q \sim \mathrm{N}\left(\mathbf{0} \ , \ \mathbf{I}\right)$,

The state estimate and estimate error vectors can be expressed using the measurement equation 60 as:

$$\hat{\mathbf{x}}_{Q|Q} = \mathbf{S}_{Q^*} \mathbf{z}_{Q^*} \quad , \quad \delta \mathbf{x}_{Q|Q} = \mathbf{S}_{Q^*} \delta \mathbf{z}_Q \quad (62)$$

where

$$\mathbf{S}_{Q^*} = \left(\mathbf{H}_{Q^*}^T \mathbf{H}_{Q^*} \right)^{-1} \mathbf{H}_{Q^*}^T \quad (63)$$

The vector $\delta \mathbf{z}_Q$ can be expressed as a sum of two orthogonal complements:

$$\delta \mathbf{z}_Q = \delta \mathbf{z}_{//,Q} + \delta \mathbf{z}_{\perp,Q} , \quad (64)$$

where $\delta \mathbf{z}_{//,Q}$ is the vector component of $\delta \mathbf{z}_Q$ that belongs to the column space of $\mathbf{H}_{Q^*}$ (i.e., $\delta \mathbf{z}_{//,Q} \in \mathrm{Range}\left\{\mathbf{H}_{Q^*}\right\}$) and $\delta \mathbf{z}_{\perp,Q}$ is the vector component of $\delta \mathbf{z}_Q$ belonging to the parity space of $\mathbf{H}_{Q^*}$ (i.e., $\delta \mathbf{z}_{\perp,Q} \in \mathrm{Null}\left\{\mathbf{H}_{Q^*}^T\right\}$).

In this two-part derivation, we first show that the current-time estimate error $\delta \mathbf{x}_{q|Q}$ is only a function of $\delta \mathbf{z}_{//,Q}$, and then we prove that $\delta \mathbf{z}_{//,Q}$ cancels out in the expression of the past-time KF residual $\mathbf{r}_{k|K}$ (which is only a function of $\delta \mathbf{z}_{\perp,Q}$).

First, the current-time state estimate error can be expressed in terms of the batch vector:

$$\delta \mathbf{x}_{q|Q} = \begin{bmatrix} \mathbf{0} & \mathbf{I} \end{bmatrix} \delta \mathbf{x}_{Q|Q} . \quad (65)$$

Substituting equation 62 into 65 and using the definition of equation 64 yields:

$$\delta \mathbf{x}_{q|Q} = \begin{bmatrix} \mathbf{0} & \mathbf{I} \end{bmatrix} \mathbf{S}_{Q^*} \left(\delta \mathbf{z}_{//,Q} + \delta \mathbf{z}_{\perp,Q} \right) . \quad (66)$$

Considering the definition of $\mathbf{S}_{Q^*}$ in equation 63, and because $\delta \mathbf{z}_{\perp,Q}$ is orthogonal to the columns of $\mathbf{H}_{Q^*}$ the product $\mathbf{H}_{Q^*}^T \delta \mathbf{z}_{\perp,Q}$ is zero. The result is then

$$\delta \mathbf{x}_{q|Q} = \begin{bmatrix} \mathbf{0} & \mathbf{I} \end{bmatrix} \mathbf{S}_{Q^*} \delta \mathbf{z}_{//,Q} . \quad (67)$$

The second part of the derivation aims at expressing past time KF residuals $\mathbf{r}_{k|K}$ as a function of batch measurement error vector components $\delta \mathbf{z}_{//,Q}$ and $\delta \mathbf{z}_{\perp,Q}$. The truncated batch residual vector is expressed using equations 4 and 11 for the truncated batch represented in

Fig. 1 (there are no complications in the normalization step – indicated by '*' subscripts – because $\mathbf{V}_Q$ is block diagonal):

$$\mathbf{r}_{K|K} = \left(\mathbf{I} - \mathbf{H}_{K^*}\mathbf{S}_{K^*}\right)\mathbf{z}_{K^*} \tag{68}$$

which can also be written as (known result):

$$\mathbf{r}_{K|K} = \left(\mathbf{I} - \mathbf{H}_{K^*}\mathbf{S}_{K^*}\right)\delta\mathbf{z}_K \tag{69}$$

In addition, the relationship between truncated and full batch measurement vectors is captured in the following equation:

$$\delta\mathbf{z}_K = \begin{bmatrix}\mathbf{I} & \mathbf{0}\end{bmatrix}\delta\mathbf{z}_Q \tag{70}$$

Substituting equation 70 into 69 and using the definition in 64 yields

$$\mathbf{r}_{K|K} = \left(\mathbf{I} - \mathbf{H}_{K^*}\mathbf{S}_{K^*}\right)\begin{bmatrix}\mathbf{I} & \mathbf{0}\end{bmatrix}\left(\delta\mathbf{z}_{//,Q} + \delta\mathbf{z}_{\perp,Q}\right) \tag{71}$$

We now show that:

$$\left(\mathbf{I} - \mathbf{H}_{K^*}\mathbf{S}_{K^*}\right)\begin{bmatrix}\mathbf{I} & \mathbf{0}\end{bmatrix}\delta\mathbf{z}_{//,Q} = \mathbf{0} \tag{72}$$

Since $\delta\mathbf{z}_{//,Q}$ belongs to the range of $\mathbf{H}_{Q^*}$, it can be expressed as

$$\delta\mathbf{z}_{//,Q} = \mathbf{H}_{Q^*}\mathbf{u}, \qquad \mathbf{u} \in \mathbb{R}^{m_Q} \tag{73}$$

where $\mathbf{u}$ is a $m_Q \times 1$ vector of real numbers. In addition, refer to Fig. 1 to see that $\mathbf{H}_{Q^*}$ can be partitioned as:

$$\mathbf{H}_{Q^*} = \begin{bmatrix}\mathbf{H}_{K^*} & \mathbf{0} \\ \mathrm{X} & \mathrm{X}\end{bmatrix} \tag{74}$$

where 'X' indicates block matrices that are not directly relevant to this derivation. Substituting equation 74 into 73 and substituting the result into the left-hand-side of equation 72 yields:

$$\left(\mathbf{I} - \mathbf{H}_{K^*}\mathbf{S}_{K^*}\right)\begin{bmatrix}\mathbf{I} & \mathbf{0}\end{bmatrix}\begin{bmatrix}\mathbf{H}_{K^*} & \mathbf{0} \\ \mathrm{X} & \mathrm{X}\end{bmatrix}\mathbf{u} \tag{75}$$

which simplifies to

$$\left(\mathbf{I} - \mathbf{H}_{K^*}\mathbf{S}_{K^*}\right)\begin{bmatrix}\mathbf{H}_{K^*} & \mathbf{0}\end{bmatrix}\mathbf{u} \tag{76}$$

Because

$$\mathbf{S}_{K^*}\mathbf{H}_{K^*} = \mathbf{I} \tag{77}$$

we proved that equation 72 is satisfied (as mentioned when establishing equation 68, the definition of $\mathbf{S}_{K^*}$ is the same as $\mathbf{S}_{Q^*}$ in equation 63 but applied to the normalized, truncated batch equation). Therefore back to equation 71, we have established that:

$$\mathbf{r}_{K|K} = \left(\mathbf{I} - \mathbf{H}_{K^*}\mathbf{S}_{K^*}\right)\begin{bmatrix}\mathbf{I} & \mathbf{0}\end{bmatrix}\delta\mathbf{z}_{\perp,Q} \tag{78}$$

Finally, from equations (67) and (78), it is clear that the current-time estimate error $\delta\mathbf{x}_{q|Q}$ and the past time KF residual vectors $\mathbf{r}_{k|K}$ (at any iteration *k*) are derived from orthogonal components of the full batch error vector $\delta\mathbf{z}_Q$.

REFERENCES

[1] Greenspan, R., "GPS and Inertial Integration," *The Global Positioning System: Theory and Applications*, B. W. Parkinson, J. J. Spilker, Jr., P. Axelrad, P. Enge, editors, AIAA Progress in Aeronautics and Astronautics Volume 163-4, Washington, DC, 1996

[2] Joerger, M., and Pervan, B., "Measurement-Level Integration of Carrier-Phase GPS and Laser-Scanner for Outdoor Ground Vehicle Navigation," *ASME Journal of Dynamic Systems, Measurement, and Control*, Vol. 131, March 2009.

[3] Chan, F-C., Joerger, M., Pervan, B., "High Integrity Stochastic Modeling of GPS Receiver Clock for Improved Positioning and Fault Detection Performance," *Proceedings of IEEE/ION PLANS 2010*, Indian Wells, CA, May 2010, pp. 1245-1257.

[4] Joerger, M., J. Christ, R. Duncan, and B. Pervan. "Integrated Design of an AGV for Improved GPS-based Path-Following Performance." *International Journal of Vehicle Design*. 42.3|4 (2006): 263-286.

[5] Lee, Y. C., "Analysis of Range and Position Comparison Methods as a Means to Provide GPS Integrity in the User Receiver," *Proceedings of the 42nd Annual Meeting of The Institute of Navigation*, Seattle, WA, June 1986, pp. 1-4.

[6] Parkinson, B. W., and Axelrad, P., "Autonomous GPS Integrity Monitoring Using the Pseudorange Residual," *NAVIGATION*, Washington, DC, Vol. 35, No. 2, 1988, pp. 225-274.

[7] Willsky, A., "A survey of design methods for failure detection in dynamic systems," *Automatica*, Vol. 12, 1976, pp. 601-611.

[8] Brown, R. G. and Hwang, Y. C., "GPS failure detection by autonomous means within the cockpit", *Proceedings of the 42nd Annual Meeting of the Institute of Navigation*, Seattle, WA, June 1986, pp. 5-12.

[9] White, N. A., Maybeck, P. S., and DeVilbiss, S. L, "Detection of Interference/Jamming and Spoofing in a DGPS-Aided Inertial System," *IEEE Transactions on Aerospace and Electronic Systems*, Vol. 34, No. 4, October 1998, pp. 1208-1217.

[10] Chan, Steven, Speyer, Jason L., "A Sequential Probability Test for RAIM," Proceedings of the 17th International Technical Meeting of the Satellite Division of The Institute of Navigation (ION GNSS 2004), Long Beach, CA, September 2004, pp. 1798-1802.

[11] Willsky, A., and Jones, H., "A generalized likelihood ratio approach to the detection and estimation of jumps in linear systems," *IEEE Transactions on Automatic Control*, Vol. 21, No. 1, February 1976, pp. 108 – 112.

[12] Sukkarieh, S., Nebot, E. M., and Durrant-Whyte, H.F., "A High Integrity IMU/GPS Navigation Loop for Autonomous Land Vehicle Applications," IEEE Transactions on Robotics and Automation, Vol. 15 No. 3, June 1999, pp. 572–578.

[13] Abuhashim, Tariq S., Abdel-Hafez, Mamoun F., and Al-Jarrah, Mohammad-Ameen, "Building a Robust Integrity Monitoring Algorithm for a Low Cost GPS-aided-INS System," *International Journal of Control, Automation, and Systems*, Vol. 8, No. 5, 2010., pp.1108-1122

[14] Hewitson, Steve, and Wang, Jinling, "Extended Receiver Autonomous Integrity Monitoring (eRAIM) for GNSS/INS Integration," *Journal of Surveying Engineering*, Vol. 136, No. 1, February 2010, pp. 13-22.

[15] Diesel, John, Luu, Sherry, "GPS/IRS AIME: Calculation of Thresholds and Protection Radius Using Chi-Square Methods," *Proceedings of the 8th International Technical Meeting of the Satellite Division of The Institute of Navigation (ION GPS 1995)*, Palm Springs, CA, September 1995, pp. 1959-1964.

[16] Bakhache, Bacem, "A Sequential RAIM Based on the Civil Aviation Requirements,' *Proceedings of the 12th International Technical Meeting of the Satellite Division of The Institute of Navigation (ION GPS 1999)*, Nashville, TN, September 1999, pp. 1201-1210

[17] Clot, A., Macabiau, C., Nikiforov, I., Roturier, B., "Sequential RAIM Designed to Detect Combined Step Ramp Pseudo-Range Error," *Proceedings of the 19th International Technical Meeting of the Satellite Division of The Institute of Navigation (ION GNSS 2006)*, Fort Worth, TX, September 2006, pp. 2621-2633.

[18] Brenner, Mats, "lntegrated GPS/lnertial Fault Detection Availability," *Proceedings of the 8th International Technical Meeting of the Satellite Division of The Institute of Navigation (ION GPS 1995)*, Palm Springs, CA, September 1995, pp. 1949-1958.

[19] Joerger, Mathieu, Gratton, Livio, Pervan, Boris, Cohen, Clark E., "Analysis of Iridium-Augmented GPS for Floating Carrier Phase Positioning", *NAVIGATION*, Vol. 57, No. 2, Summer 2010, pp. 137-160.

[20] Crassidis, J., and J. Junkins,. *Optimal Estimation of Dynamic Systems*, Boca Raton, FL: Chapman & Hall/CRC, 2004.

[21] Sturza, M, "Navigation System Integrity Monitoring Using Redundant Measurements," *NAVIGATION: Journal of the Institute of Navigation*, Washington, DC, Vol. 35 No. 4, 1988, pp. 69-87.

[22] Pervan, B., "Navigation integrity for aircraft precision landing using the global positioning system," *Ph.D. Dissertation*, Stanford University, March 1996.

[23] Joerger, M., Pervan, B., "Sequential Residual-Based RAIM," *Proceedings of the 23rd International Technical Meeting of The Satellite Division of the Institute of Navigation (ION GNSS 2010)*, Portland, OR, September 2010, pp. 3167-3180.

[24] Ropokis, G., Rontogiannis, A., and Mathiopoulos, P., "Quadratic forms in normal rvs: Theory and applications to OSTBC over Hoyt fading channels," *IEEE Transactions on Wireless Communication*s, Vol. 7, No. 12, 2008, pp.5009 - 5019.

[25] Davies, Robert B., "Algorithm AS 155: The Distribution of a Linear Combination of $\chi 2$ Random Variables," *Journal of the Royal Statistical Society, Series C (Applied Statistics)*, Vol. 29, No. 3 (1980).

[26] Joerger, M., Neale, J., Pervan, B., Datta-Barua, S., "Measurement Error Models and Fault-Detection Algorithms for Multi-Constellation Navigation Systems," *Proceedings of IEEE/ION PLANS 2010*, Indian Wells, CA, May 2010, pp. 927-946.